MANEUVER SIMULATIONS OF FLEXIBLE SPACECRAFT BY SOLVING TPBVP

Peter M. Bainum
Distinguished Professor of Aerospace Engineering
Department of Mechanical Engineering
Howard University, Washington D.C.

and

Feiyue Li
Graduate Research Assistant
Department of Mechanical Engineering
Howard University, Washington D.C.

4th NASA Workshop on Computational Control of Flexible Aerospace Systems

Kingsmill Resort, Williamsburg, Virginia
July 11-13, 1990

MANEUVER SIMULATIONS OF FLEXIBLE SPACECRAFT BY SOLVING TPBVP*

Feiyue Li and Peter M. Bainum
Department of Mechanical Engineering
Howard University, Washington D.C.

SUMMARY

The optimal control of large-angle rapid maneuvers and vibrations of a Shuttle-mast-reflector system is considered. The nonlinear equations of motion are formulated by using Lagrange's formula, with the mast modeled as a continuous beam. The nonlinear terms in the equations come from the coupling between the angular velocities, the modal coordinates, and the modal rates. Pontryagin's Maximum Principle is applied to the slewing problem, to derive the necessary conditions for the optimal controls, which are bounded by given saturation levels. The resulting two-point boundary-value problem (TPBVP) is then solved by using the quasilinearization algorithm and the method of particular solutions. In the numerical simulations, the structural parameters and the control limits from the Spacecraft Control Laboratory Experiments (SCOLE) are used.

In the two-dimensional (2-D) case, only the motion in the plane of an Earth orbit or the single-axis slewing motion will be discussed. The effects of the structural offset connection, the so-called axial shortening, and the gravitational torque on the slewing of a flexible spacecraft in Earth orbit is considered. In the case of three-dimensional (3-D) slewing, the mast is modeled as a continuous beam subject to 3-D deformations. The numerical results for both the linearized system and the nonlinear system are presented to compare the differences in their time responses.

INTRODUCTION

Future space missions require large-angle rotational (attitude), 3-dimensional maneuvering ("slew") of a large flexible spacecraft in target acquisition, target tracking, and surveying multiple targets, etc. The whole spacecraft system may be composed of multibodies, including the "rigid" parts involving large relative movements and its flexible parts undergoing "small" deformations. The motions of the system for these space activities are best described by nonlinear equations instead of the "linearized" or linear equations. Many authors have considered the problem of large-angle rapid maneuvers of flexible spacecraft (refs. 1-8). The direct application of Pontryagin's maximum principle to this problem has been applied by many authors (refs. 1-3, 6-8). Most of these researches are concentrated on the 2-D slewing problem, except ref. 8, a recent result for the 3-D slewing of the SCOLE.

2-D Slewings

In ref. 6, the rapid slewing of the 2-D SCOLE has been considered. It is

* Research supported by NASA Grant NSG-1414.

observed that (ref. 6) the time response history of the nonlinear system has a shift from that of the linearized system; the reason for this is mainly due to the structural offset (ref. 7).

The so called axial shortening effect of a beam induced by its transverse displacement has been brought to attention by some authors (Refs. 1-3, 9). Although the shortening terms have been included in the equations (Refs. 1-3), their effect on the slew lacked quantitative analysis; specifically, the numerical examples with and without these terms were not provided. On the other hand, a numerical example in Ref. 9 shows that large differences do result between models with and without the shortening effect. But the numerical example is only for an uncontrolled dynamical response case and the main body's motion is prescribed. In ref. 7, therefore, the shortening terms are considered in the formulation of the equations of motion and numerical examples both with and without these terms are presented to compare the difference between them. Also in ref. 7, the gravitational torque terms are modeled and included in the equations to show their effect on the slewing motion.

3-D Slewings

The direct solution of the open-loop TPBVP for 3-D slews of flexible spacecraft resulted in numerical problems with rank-deficient matrices as stated in ref. 5. However, a different numerical method may be used to overcome this difficulty. In ref. 8, the problem has been solved successfully by using the quasilinearization algorithm and the method of particular solutions for 3-D slews of the asymmetrical flexible SCOLE configuration.

The open-loop slewing approach has several obvious distinct properties. First, the control law is easy to implement in practice for both ground tests and space flight tests. Second, the open-loop solution may serve as a good reference for the feedback control law design, as proposed in refs. 4-5, in which the open-loop solution for a rigid (instead of a flexible) spacecraft is used as the nominal reference trajectory. As an extension to refs. 4-5, it may be helpful if the open-loop solution for the 3-D slew of a flexible spacecraft system could also be used as a nominal reference solution. In addition, through the present study, we can also see how different are the responses of the nonlinear system from those of the linearized system.

In the present report, we will summarize most of the results obtained in refs. 7-8. At the same time, the detailed numerical techniques (briefly mentioned in refs. 7-8) for solving the nonlinear TPBVP will be discussed. Numerical examples are presented to illustrate the use of the techniques and the numerical problems associated with the calculations will be discussed.

EQUATIONS OF THE SYSTEMS

System Configurations

The 2-D and 3-D models of the orbiting SCOLE are shown in figures 1 and 2 , respectively. The Shuttle and the reflector are assumed to be rigid bodies. One end of the flexible mast is fixed to the Shuttle at its mass center, o_s, while the other end is firmly connected to the reflector at an offset point, a_r (x_r in the 2-D

case). Three Euler angles (θ_1, θ_2, θ_3) (θ in the 2-D case) or four quaternions are used to describe the attitude of the Shuttle with respect to an orbital reference system.

The 3-D deformation of the mast consists of two bending deflections $U(z,t)$ and $V(z,t)$ in the x-z and y-z planes, respectively, and torsion $\phi(z,t)$ about the z axis. It is assumed that these deformations are small as compared with the length of the mast and can be expressed by the following modal superposition formulas (ref. 10):

$$U(z,t)=\sum_i \xi_i(z)\alpha_i(t), \quad V(z,t)=\sum_i \eta_i(z)\alpha_i(t), \quad \phi(z,t)=\sum_i \zeta_i(z)\alpha_i(t), \tag{1}$$

where ξ_i, η_i, and ζ_i are modal shape function vector components normalized by a common factor, and α_i is a scaled modal amplitude associated with the ith mode. In the 2-D case, only the first equation is used.

The free vibration of this structure can be considered as a space free-free beam vibration problem with boundary conditions including the masses and moments of inertia of the Shuttle and the reflector. The partial differential equation formulation for this problem (refs. 10-11) can be solved by using the separation of variables method. Note that the natural frequencies and modal functions of the 2-D structure are different from those of the 3-D structure.

2-D Dynamical Equations

After developing the kinetic energy and potential energy, we can obtain the dynamical equations of the 2-D structure in the following matrix form (ref. 7):

$$\left[\begin{array}{c|c} I+2\alpha^T m_a+\alpha^T M_2\alpha & (m_2+M_4\alpha)^T \\ \hline m_2+M_4\alpha & M_3 \end{array}\right]\left[\begin{array}{c} \ddot{\theta} \\ \ddot{\alpha} \end{array}\right]=\left[\begin{array}{c} -2\dot{\theta}\dot{\alpha}^T(m_a+M_2\alpha)-\dot{\alpha}^T M_5\dot{\alpha}-\partial V_g/\partial\theta+Q_\theta \\ \hline -2\dot{\theta}M_a\dot{\alpha}+\dot{\theta}^2(m_a+M_2\alpha)-K\alpha-\partial V_g/\partial\alpha+Q_\alpha \end{array}\right] \tag{2}$$

where α is the n×1 modal amplitude vector, n is the number of flexible modes; M_i(i=2,3,4,5) and M_a are constant n×n matrices; m_a and m_2 are n×1 constant vectors; K is the n×n constant diagonal stiffness matrix; V_g is the gravitational energy of the system which is a function of the orbital rate, ω_0, rotation angle, θ, and the deformation amplitude, $\alpha(t)$; and Q_θ, Q_α are the generalized forces produced by the controls associated with θ and α, respectively.

In equation (2), the elements of the vector, m_a, and the matrices, M_a, M_4, and M_5 have a common factor x_r, the offset. In another words, x_r=0 results in m_a=0, etc. The effect of this structural offset on the slewing is analyzed by changing the value of x_r (from 0 to 32.5 ft). Of course, different x_r imply different natural frequencies and modes. The frequencies decrease as the offset distance increase.

The axial shortening of the beam due to the geometric deformation is also considered by adding a shortening term

$$\Delta z=\frac{1}{2}\int_0^z\left(\frac{\partial U}{\partial z}\right)^2 dz$$

into the formulation. Apparently, Δz is a second order term in the modal amplitude, α. The shortening term is involved in the matrices M_2, M_5 in equation (2).

If we distinguish the terms on the right side of equation (2) according to their order in α and $\dot{\alpha}$, we can see that m_a and M_a are involved in the lower order terms, while M_2 and M_5 contribute to the higher order terms. Therefore, for moderate nonzero values of x_r and small-deformation slews, the influence of the structural offset can be greater than the shortening effect. The linearized equations can be obtained by neglecting all nonlinear terms,

$$\left[\begin{array}{c:c} I & m_2^T \\ \hdashline m_2 & M_3 \end{array}\right]\left[\begin{array}{c}\ddot{\theta}\\ \ddot{\alpha}\end{array}\right]=\left[\begin{array}{c}0\\ \hdashline -K\alpha\end{array}\right]+\left[\begin{array}{c}-\partial V_g/\partial\theta+Q_\theta\\ \hdashline -\partial V_g/\partial\alpha+Q_\alpha\end{array}\right]_{LIN} \tag{3}$$

where "LIN" refers to constant and linear terms. Note that on the right side of equation (3), both the structural offset and the shortening terms disappear. This means that by using the linearized equations of motion, we may lose some important information such as the terms associated with the structural offset about the original system.

3-D System Equations

The dynamic equations for the 3-D system can be obtained, by using the Lagrangian method, in the following state form (ref. 8):

$$\dot{y}=\left[\begin{array}{c}\dot{\omega}\\ \dot{\beta}\end{array}\right]=(A+\bar{B}_\alpha)\bar{\bar{\omega}}+(\bar{C}_\beta)\omega+D\alpha+(E+\bar{F}_\alpha)u \tag{4}$$

where α is the $n\times 1$ modal amplitude vector, $\beta=\dot{\alpha}$ is the modal rate vector, ω is the 3×1 angular velocity vector of the Shuttle, $\bar{\bar{\omega}}$ is a 6×1 vector defined by

$$\bar{\bar{\omega}}=\left[\omega_1^2\quad \omega_2^2\quad \omega_3^2\quad \omega_2\omega_3\quad \omega_3\omega_1\quad \omega_1\omega_2\right]^T$$

and u is the 9×1 control vector:

$$u=[f_{1x}\ f_{1y}\ f_{1z}\,|\,f_{2x}\ f_{2y}\,|\,f_{3x}\ f_{3y}\,|\,f_{4x}\ f_{4y}]^T.$$

$A_{(3+n)\times 6}$, $D_{(3+n)\times n}$, and $E_{(3+n)\times 9}$, are constant matrices. Also, $(\bar{B}_\alpha)_{(3+n)\times 6}$, $(\bar{C}_\beta)_{(3+n)\times 3}$, $(\bar{F}_\alpha)_{(3+n)\times 9}$, are defined as

$$\bar{B}_\alpha=[B_1\alpha\ |\ B_2\alpha\ |\cdots|\ B_6\alpha],\quad \bar{C}_\beta=[C_1\beta\ |\ C_2\beta\ |\ C_3\beta],\quad \bar{F}_\alpha=[F_1\alpha\ |\ F_2\alpha\ |\cdots|\ F_9\alpha]$$

where B_i, C_i, F_i are all (3+n)×n constant matrices.

Note that in the development of equations (4), a constant inertia (mass) matrix has been assumed for convenience. Meanwhile, all the second and higher order terms of the flexible variables (α and $\dot{\alpha}$) are abandoned in the final equations. But all nonlinear terms ($\bar{\bar{\omega}}$) representing the rigid body motion are retained.

Clearly, the dynamic equations for the rigidized spacecraft can be obtained by deleting all terms related with α and β, that is,

$$\dot{\omega} = \bar{A}\,\bar{\bar{\omega}} + \bar{E}\,u \tag{5}$$

where $\bar{A}$ and $\bar{E}$ are 3×6 and 3×9 constant matrices, respectively.

A linearized form of Equation (4) can also be obtained by deleting all nonlinear terms,

$$\dot{y} = D\alpha + Eu \tag{6}$$

By using the quaternion vector $q=[q_0\ q_1\ q_2\ q_3]^T$, the kinematic equations can be expressed as

$$\dot{q} = \frac{1}{2}\,\tilde{\underline{\omega}}\,q, \qquad \text{where} \quad \tilde{\underline{\omega}} = \begin{bmatrix} 0 & -\omega_1 & -\omega_2 & -\omega_3 \\ \omega_1 & 0 & \omega_3 & -\omega_2 \\ \omega_2 & -\omega_3 & 0 & \omega_1 \\ \omega_3 & \omega_2 & -\omega_1 & 0 \end{bmatrix} \tag{7}$$

OPTIMAL CONTROL-NECESSARY CONDITIONS

For the 3-D slewing problem, we use the following quadratic cost functional,

$$J=\frac{1}{2}\int_0^{t_f}(\alpha^T Q_1\alpha + \omega^T Q_2\omega + \beta^T Q_3\beta + u^T Ru)dt \tag{8}$$

where Q_i, and R are weighting matrices, t_f is the given slewing time. The magnitudes of the controls, u, are bounded,

$$|u_i| \le u_{ib}, \qquad i=1,\cdots, 9. \tag{9}$$

The Hamiltonian of the system is,

$$H=\frac{1}{2}(\alpha^T Q_1\alpha + \omega^T Q_2\omega + \beta^T Q_3\beta + u^T Ru + p^T\tilde{\underline{\omega}}q)+\gamma^T\beta+\lambda^T[(A + \bar{B}_\alpha)\bar{\bar{\omega}} + (\bar{C}_\beta)\omega + D\alpha + (E + \bar{F}_\alpha)u]$$

where p, γ, and $\lambda=[\lambda_1\ \lambda_2]^T$ are the costate vectors associated with q, α, ω, and β, respectively. By using the Maximum Principle, the necessary conditions for the unrestricted optimal control problem are the dynamical equations (4, 7) plus the following differential equations for the costates,

$$\dot{p} = -\frac{\partial H}{\partial q} = \frac{1}{2}\tilde{\omega}\, p, \qquad \dot{\gamma} = -\frac{\partial H}{\partial \alpha} = -Q_1\alpha - D^T\lambda - (\bar{B}_\alpha^T\lambda)\bar{\omega} - (\bar{F}_\alpha^T\lambda)u \tag{10a,b}$$

$$\dot{\lambda}_1 = -\frac{\partial H}{\partial \omega} = -Q_2\omega - \frac{1}{2}[q]p - [\lambda^T(A+\bar{B}_\alpha)]\omega - (\bar{C}_\beta)^T\lambda, \qquad \dot{\lambda}_2 = -\frac{\partial H}{\partial \beta} = -Q_3\beta - \gamma - (\bar{C}_\beta^T\lambda)\omega \tag{10c,d}$$

and the optimal control,

$$\frac{\partial H}{\partial u} = 0, \quad \Longrightarrow \quad u = -R^{-1}(E+\bar{F}_\alpha)^T\lambda \tag{11}$$

The control law (11) is then modified by consideration of the saturations (9):

$$u_i = \left\{ \begin{array}{ll} -u_{ib}, & \text{if } u_{ic} \le -u_{ib} \\ u_{ib}, & \text{if } u_{ic} \ge u_{ib} \end{array} \right\}, \quad \begin{array}{l} \text{otherwise,} \\ u_i = u_{ic} = -[R^{-1}(E+\bar{F}_\alpha)^T\lambda]_i \\ \qquad\qquad i = 1, \ldots, 9. \end{array} \tag{12}$$

The same type of cost functional has been used for the 2-D slew problem. Therefore, the associated necessary conditions are similar to equations (10) and (12).

Two-Point Boundary-Value Problem (TPBVP)

One way of obtaining the optimal control law is to transform the above necessary conditions into the following TPBVP. Let x represent the state vector, and λ represent the costate vector. After substituting the control expressions (12) into equations (4) and (10b), one can obtain two sets of ordinary differential equations for the states and the costates,

$$\dot{x} = f_1(x, \lambda)_{(7+2n)\times 1} \tag{13a}$$

$$\dot{\lambda} = f_2(x, \lambda)_{(7+2n)\times 1} \tag{13b}$$

with the following boundary conditions,

$$x(0) \text{ and } x(t_f) \text{ prescribed}, \quad \lambda(0) \text{ and } \lambda(t_f) \text{ unknown}. \tag{14}$$

Due to the known boundary conditions being specified at the two ends of the slewing time, this problem is usually called the two-point boundary-value problem. This kind of split boundary conditions usually result from the large-angle maneuver requirements, in which the initial ($t=0$) and final ($t=t_f$) states of the system are specified. By solving this problem, we can obtain the optimal control (based on the necessary conditions). The often used solution strategy is to change the boundary value problem to the initial value problem, i.e., find $\lambda(0)$, the missing initial costates. Once $\lambda(0)$ is obtained, one can solve the equations (13) as an initial value problem by using any numerical integration method. However, owing to the nonlinearity of the equations, there is generally no analytical solution to this problem or simple numerical method to obtain the solution except for some very simple cases such as the linear time-invariant case. The numerical iteration method is the general approach to the this problem.

To start an iteration process, one usually needs an initial guess of $\lambda^{(0)}(0)$. Then, equations (13) or their equivalent form (the linearized version of (13)) are

solved and a $x^{(0)}(t_f)$ is obtained. Based on the difference $\Delta x(t_f)=x^{(0)}(t_f)-x(t_f)$, the correction to $\lambda(0)$, $\Delta\lambda(0)$, is obtained. This gives us a new initial value of $\lambda(0)$, $\lambda^{(1)}(0)$. Hence, the next iteration begins. The iteration process can be terminated when $|\lambda^{(k+1)}(0)-\lambda^{(k)}(0)|$ is less than a given error limit. One can see immediately that if the beginning guess $\lambda^{(0)}(0)$ is close to the true value (converged value) of $\lambda(0)$, the solution will converge and less iterations are needed. However, a "good" guess of $\lambda(0)$ is often difficult to obtain for the general nonlinear problems.

Therefore, the effort for solving the TPBVP is two fold. The first is try to establish a good iteration (correction) method with a wide convergence interval so that it can guarantee convergence even for a "poor" initial guess. The other is try to find a "good" initial guess based on the characteristics of the practical problem and using some simplified mathematical models. In this report, we use the quasilinearization method. We also use the solution of $\lambda(0)$ from the simplified linear, time-invariant model of the system as the initial guess for starting the iteration process.

Linear and Time-Invariant TPBVP

For linear, time-invariant versions of equations (13) (refs. 1-3),

$$\dot{z}=Az, \quad \text{where } z^T=[x^T, \lambda^T] \tag{15}$$

its transition matrix (constant exponential matrix),

$$e^{At_f}=\begin{bmatrix} A_{11} & A_{12} \\ A_{21} & A_{22} \end{bmatrix}$$

can be used to obtain the initial costates (closed form solution):

$$\lambda(0)=A_{12}^{-1}[x(t_f)-A_{11}x(0)] \tag{16}$$

Nonlinear TPBVP

The continuation (relaxation) process (to increase the participation of the nonlinearity in the solution) and the differential correction (for determination of the initial costate variables) have been used in references 1-3 for the 2-D slewing problem. However, as stated in ref. 5, the extension of these techniques to the 3-D slewing problem has encountered a numerical problem: rank deficiency.

In references 6-8, the quasilinearization method has been successfully used. In this method, one needs to linearize the differential equations (13),

$$\dot{z}=g(z), \quad \text{where } z^T=[x^T, \lambda^T], \quad g^T=[f_1^T, f_2^T] \tag{17}$$

about an approximate solution of this equation in the following form (a series of linearized, time-variant, nonhomogeneous equations):

$$\dot{z}^{(k+1)}=(\partial g/\partial z)z^{(k+1)} + h(z^{(k)}) \tag{18}$$

where $z^{(k)}$ is the kth solution of the same linearized equation. It is also the kth approximate solution of the original nonlinear equations (17). Here, the boundary conditions, (14), are naturally adopted as the boundary conditions of the linearized equations, (18). The control expressions, (11), also need to be linearized (ref. 12):

$$u^{(k+1)}=u^{(k)}-R^{-1}[\bar{F}(\Delta\alpha)]^T\lambda^{(k)}-R^{-1}[E+\bar{F}(\alpha^{(k)})]^T\Delta\lambda \tag{19}$$

where $\Delta\alpha=\alpha^{(k+1)}-\alpha^{(k)}$, and $\Delta\lambda=\lambda^{(k+1)}-\lambda^{(k)}$. By assuming that

$$u^{(k)}=-R^{-1}[E+\bar{F}(\alpha^{(k)})]^T\lambda^{(k)} \tag{20}$$

for the unbounded control case, equation (19) can be rewritten as,

$$u^{(k+1)}=-R^{-1}[\bar{F}(\Delta\alpha)]^T\lambda^{(k)}-R^{-1}[E+\bar{F}(\alpha^{(k)})]^T\lambda^{(k+1)} \tag{21}$$

However, in the bounded control case, equations (12) are considered, that is,

$$u_i^{(k)}=\begin{cases} -u_{ib} \quad \text{or} \quad u_{ib} \\ -\{R^{-1}[E+\bar{F}(\alpha^{(k)})]^T\lambda^{(k)}\}_i \end{cases} \tag{22}$$

Accordingly, at the (k+1)st step, $u^{(k+1)}$ can be determined by

$$u_i^{(k+1)}=\begin{cases} -u_{ib} \quad \text{or} \quad u_{ib}, \quad \text{if} \quad |\{R^{-1}[E+\bar{F}(\alpha^{(k)})]^T\lambda^{(k)}\}_i| \geq u_{ib} \\ -\{R^{-1}[\bar{F}(\Delta\alpha)]^T\lambda^{(k)}-R^{-1}[E+\bar{F}(\alpha^{(k)})]^T\lambda^{(k+1)}\}_i \end{cases} \tag{23}$$

So far, an iteration process is formed. In each iteration, only a linear TPBVP is solved. It is this property that gives this approach the name quasilinearization method.

The linear TPBVP can be solved by many ready-made methods. One of the frequently used algorithms is the method of particular solutions (ref. 13). Let m represent the number of the states (also the costates). Equations (18) can also be rewritten in the following form,

$$\dot{x}(t)=G(t)x(t)+H(t)\lambda(t), \quad \dot{\lambda}(t)=I(t)x(t)+J(t)\lambda(t) \tag{24a,b}$$

From the theorem of the linear system, any solution equation (24a) can be expressed as the linear combination of its m+1 particular solutions, i.e.,

$$x(t)=\sum_{i=1}^{m+1} c_i x^i(t), \quad \text{as long as} \sum_{i=1}^{m+1} c_i=1 \tag{25}$$

where c_i are constants and $x^i(t)$ are the ith particular solution vectors. The method begins by integrating equations (24a, b) forward m+1 times, with the initial conditions,

$$z^1(0)=\begin{bmatrix} x(0) \\ 1 \\ 0 \\ 0 \\ \vdots \\ 0 \end{bmatrix},\ z^2(0)=\begin{bmatrix} x(0) \\ 0 \\ 1 \\ 0 \\ \vdots \\ 0 \end{bmatrix},\ \ldots,\ z^m(0)=\begin{bmatrix} x(0) \\ 0 \\ 0 \\ \vdots \\ 0 \\ 1 \end{bmatrix},\ \text{and}\ z^{m+1}(0)=\begin{bmatrix} x(0) \\ 0 \\ 0 \\ 0 \\ \vdots \\ 0 \end{bmatrix}.$$

This gives us m+1 particular solutions, $x^1(t)$, $x^2(t)$, $\cdots$, $x^{m+1}(t)$. Substituting these solutions into equations (25), and setting $t=t_f$, we have

$$\sum_{i=1}^{m+1} c_i x^i(t_f)=x(t_f), \qquad \sum_{i=1}^{m+1} c_i=1 \tag{26}$$

This is a set of m+1 algebra equations for m+1 unknown constants, c_i. By assuming the existence of inverse of the coefficient matrix, we can obtain the solution, $c=[c_1\ c_2\ \cdots\ c_m]^T$ and c_{m+1}. By doing the following manipulation,

$$z(0)=\sum_{i=1}^{m+1} c_i z^i(0)=\begin{bmatrix} \sum_{i=1}^{m+1} c_i x^i(0) \\ c_1 \\ c_2 \\ \vdots \\ c_m \end{bmatrix}=\begin{bmatrix} x(0) \\ c_1 \\ c_2 \\ \vdots \\ c_m \end{bmatrix}$$

one immediately realizes that $c=\lambda(0)$, the missing initial costates.

NUMERICAL RESULTS

2-D Slews

The parameters of the orbiting SCOLE (refs. 10-11) are used. The orbital angular rate is chosen as ω_0=0.001 (rad/s) (orbital altitude $\approx$ 981 km). The first three natural frequencies used here are:

0.3365257, 2.062547, 5.316669 (hz), for x_r=0;
0.3199540, 1.287843, 4.800169 (hz), for x_r=32.5 (ft) (same as ref. 10)

All simulations are 90 degree rest-to-rest slews and can be represented by:

Case 1 x_r=0, $\bar{u}=u_1$, R=1E-6, t_f=27.6 (s)
Case 2 x_r=0, $\bar{u}=[u_1\ u_2\ u_3\ u_4]^T$, R=DIAG(1E-6, .15, .21, 1E-4), t_f=8.196 (s)
Case 3 x_r=32.5 (ft), $\bar{u}=u_1$, R=1E-6, t_f=27.6 (s)
Case 4 x_r=32.5 (ft), $\bar{u}=[u_1\ u_2\ u_3\ u_4]^T$, R=DIAG(1E-6, .15, .21, 1E-4), t_f=8.196 (s)

Figs. 3a-g display the time histories of $\theta(t)$, $u(L,t)$, $\phi(L,t)$, $\bar{u}(t)$ for Case 4. Clearly, the response of $\theta(t)$ for both linear and nonlinear systems are very close. However, there exist some differences between the two systems in $u(L,t)$, $\phi(L,t)$ and the controls, u. The difference is primarily due to the offset x_r (here, x_r=32.5 ft). When x_r=0, this difference can be reduced markedly, regardless of whether the shortening effect and gravitation are considered. It is also interesting to know that the controls have large differences only around the mid-slew-time.

Table 1 lists the maximum (minimum) values for the displacement, $u(L,t)$, and angle, $\phi(L,t)$, of the beam during the associated slews for all cases. The first line in each case lists the results for the linearized system, while all remaining lines represent those for the nonlinear system with different considerations. For example, ΔL=0 means the shortening effect is not considered. The last column gives the largest relative displacement error, with respect to the linear results, based on

$$(e_{Disp})_* = \text{Max}\left(|MAX_* - MAX_{LIN}| / |MAX_{LIN}|,\ |MIN_* - MIN_{LIN}| / |MIN_{LIN}| \right)$$

Nonlinear System vs. Linearized System First, let us examine line 1 and line 2 in each case. In Case 1, since no offset, the differences between the two lines are very small. In Case 2, where more controllers are used and the slewing time is shortened, the differences increase symmetrically ($|MAX| = |MIN|$), in spite of x_r=0. Case 3 uses the same slewing conditions as used in Case 1, except x_r=32.5 ft. This offset shifts the envelop of the response downward and results in a larger relative displacement error than that in Case 2. Case 4 is the combination of Cases 2 and 3. The shift now is upward which is due to the inclusion of more controllers. When more controllers are used (Ref. 3), the phase of the response reverses, so do the maximum (minimum) amplitudes.

Shortening Effect By comparing line 2 and line 3 in each case, we can see that the shortening terms (1) reduce the amplitude (Cases 2 and 3); (2) increase the amplitude (Case 4); and shift the response upward (Cases 3 and 4). These observations coincide with the fact that Δz only results in a second order effect as compared with the offset effect.

Gravitational Effect By observing lines 3 and 4, we can conclude that the addition of the gravitational torques into the equations of motion has a very small effect on the slew, although they shift the response downward. This is because the orbital rate is much smaller than the slewing rate and the magnitude of the gravitational torque term is much smaller than that of the active control torque term.

3-D Slews

The location of the mass center of the reflector is x_r=18.75 ft, and y_r=32.5 ft. The first five natural frequencies are (hz): .2740493, .3229025, .7487723, 1.244013, 2.051804.

The numerical tests based on the previously described method have been performed for the roll-axis slews, pitch-axis slews, as well as arbitrary-axis slews. All these tests are rest-to-rest slews and the iteration process is terminated after the initial costates are reached within five digit accuracy.

The following procedure is designed to obtain the solution of the nonlinear

TPBVP (figure 4). First, the linear TPBVP based on equation (6) is solved and a nominal trajectory is produced, in which the control is unbounded and the initial costates are calculated by using the transition matrix method. Then, a converged solution for the linear TPBVP with bounded controls is obtained by iterations starting from the previously obtained trajectory. Note that the Euler angles are used in all the above computations.

Next, to obtain the starting solution for the nonlinear TPBVP, the 3 Euler angles and the 3 associated costates are transformed to the 4 quaternions and their 4 costates (from t=0 to t=t_f). Reference 14 provides us the following relationship between the quaternions, q(t) and their costates, p(t):

$$\begin{bmatrix} p_0 \\ p_1 \\ p_2 \\ p_3 \end{bmatrix} = \begin{bmatrix} d_0 & -d_1 & -d_2 & -d_3 \\ d_1 & d_0 & -d_3 & d_2 \\ d_2 & d_3 & d_0 & -d_1 \\ d_3 & -d_2 & d_1 & d_0 \end{bmatrix} \begin{bmatrix} q_0 \\ q_1 \\ q_2 \\ q_3 \end{bmatrix} \tag{27}$$

where d_i are constants. For the case $q(0)=[1\ 0\ 0\ 0]^T$, we can choose $p_0(0)=0$, $d_0=0$. Then,

$$[p_1(0)\ p_2(0)\ p_3(0)]=[d_1\ d_2\ d_3]=d^T \tag{28}$$

The vector d can be determined by

$$d= 2\ [\text{initial Euler angle costate vector}] \tag{29}$$

This result can be proved if one compares the related state and costate equations for both linear and nonlinear TPBVPs (for the case $\omega(0)=0$). After finding the q(t) by using a nonsingular transformation between q(t) and the Euler angles, $\theta_1(t)$, $\theta_2(t)$, and $\theta_3(t)$, one can use equations (27-29) to obtain p(t).

Finally, the nonlinear TPBVP is solved through the quasilinearization process and the method of particular solutions.

Case 3: Fig. 5 shows the results for a simultaneous three-axis slew (θ_1=60, θ_2=30, θ_3=45 deg). The weightings for the states are $Q_1=Q_2=Q_3=0$. In this case, The Shuttle torques (f_{1x}, f_{1y}, and f_{1z}) and the reflector forces (f_{4x}, and f_{4y}) are used. The associated weighting for the control is R=DIAG(1E-4, 1E-4, 1E-4, 0.6, 1.4-3). The slewing time, t_f, is 40 sec. The solid lines in the figures 5a-h responses of the rigidized system, equation (5), while the dotted lines represent the slew results for the flexible spacecraft.

CONCLUSION

Generally, for the 2-D case, the linearized system can predict the system dynamics very well in the slow slewing case. However, in the rapid large-angle slewing problem, the responses of the system deviate noticeably from those described

by the linearized equations if the effects of structural offset and axial shortening are included in the simulations. The structural offset (if any) results in a first order nonlinear effect. The shortening effect results in only a second order nonlinear effect and may not be considered, in the controlled simulations, unless the deformation is out of the linear range. The gravitational effect can be safely neglected in the slew motions considered here.

The application of Pontryagin's Maximum Principle to the large angle slewing maneuver problem has been extended to the slewing of a 3-D flexible spacecraft (SCOLE). A numerical simulation procedure based on the quasilinearization algorithm for solving the resulting nonlinear TPBVP has been established and tested successfully for several examples. The general nonlinear dynamical equations developed here contain all quadratic terms in the angular velocity components of the main body and their coupling with the first order modal amplitudes and modal rates. It is suggested that higher order terms be included if a further analysis is conducted. The numerical results show an important fact that the linearized system can represent the nonlinear system adequately for predicting the major motions but not as well for the secondary motions. For further research, it is recommended that the applicability of this method to more complicated systems be established.

REFERENCES

1. Turner, J.D. and Junkins, J.L.: Optimal Large-Angle Single-Axis Rotational Maneuvers of Flexible Spacecraft. Journal of Guidance and Control, vol. 3, no. 6, 1980, pp. 578-585.

2. Turner, J.D. and Chun, H.M.: Optimal Distributed Control of a Flexible Spacecraft During a Large-Angle Maneuver. Journal of Guidance, Control, and Dynamics, vol. 7, no. 3, 1984, pp. 257-264.

3. Junkins, J.L. and Turner, J.D.: Optimal Spacecraft Rotational Maneuvers. Elsevier, Amsterdam, 1986.

4. Meirovitch, L. and Quinn, R.D.: Maneuvering and Vibration Control of Flexible Spacecraft. Journal of the Astronautical Sciences, vol. 35, no. 3, 1987, pp. 301-328.

5. Chun, H.M., Turner, J.D. and Juang, J.-N.: Frequency-Shaped Large-Angle Maneuvers. Journal of the Astronautical Sciences, vol. 36, no. 3, 1988, pp. 219-234.

6. Bainum, P.M. and Li, F.: Rapid In-Plane Maneuvering of the Flexible Orbiting SCOLE. AAS/AIAA Astrodynamics Specialist Conf., Stowe, Vermont, Aug. 7-10, 1989, AAS Paper 89-422. to appear Journal of the Astronautical Sciences.

7. Li, F. and Bainum, P.M.: Effects of Structural Offset, Axial Shortening, and Gravitational Torque on the Slewing of a Flexible Spacecraft. 17th International Symposium on Space Technology and Science, Tokyo, Japan, May 20-25, 1990.

8. Bainum, P.M. and Li, F.: Optimal Large Angle Maneuvers of a Flexible Spacecraft. International Conference: Dynamics of Flexible Structures in Space, Cranfield, Bedford, UK, May 15-18, 1990.

9. Kane, T.R., Ryan, R.R., and Banerjee, A.K.: Dynamics of a Cantilever Beam Attached to a Moving Base. Journal of Guidance, Control, and Dynamics, vol. 10, no. 2, 1987, pp. 139-151.

10. Taylor, L.W. and Balakrishnan, A.V.: A Mathematical Problem and a Spacecraft Control Laboratory Experiment (SCOLE) Used to Evaluate Control Laws for Flexible Spacecraft ... NASA/IEEE Design Challenge. Proc. of the 4th VPI&SU Symposium on Dynamics and Control of Large Structures, Blacksburg, VA, June 1983. Revised Jan. 1984.

11. Robertson, D.K.: Three-Dimensional Vibration Analysis of a Uniform Beam with Offset Inertial Masses at the Ends. NASA Technical Memorandum 86393, Sept. 1985.

12. Yeo, B.P., Waldron, K.J. and Goh, B.S.: Optimal Initial Choice of Multipliers in the Quasi-linearization Method for Optimal Control Problems with Bounded Controls. Int. Journal of Control, vol. 20, no. 1, 1974, pp. 17-33.

13. Miele, A. and Iyer, R.R.: General Technique for Solving Nonlinear Two-Point Boundary-Value Problems via the Method of Particular Solutions. Journal of Optimization Theory and Applications, vol. 5, no. 5, 1970, pp. 382-399.

14. Li, F. and Bainum, P.M.: "Numerical Approach for Solving Rigid Spacecraft Minimum Time Attitude Maneuvers. Journal of Guidance, Control, and Dynamics, vol. 13, no. 1, 1990, pp. 38-45.

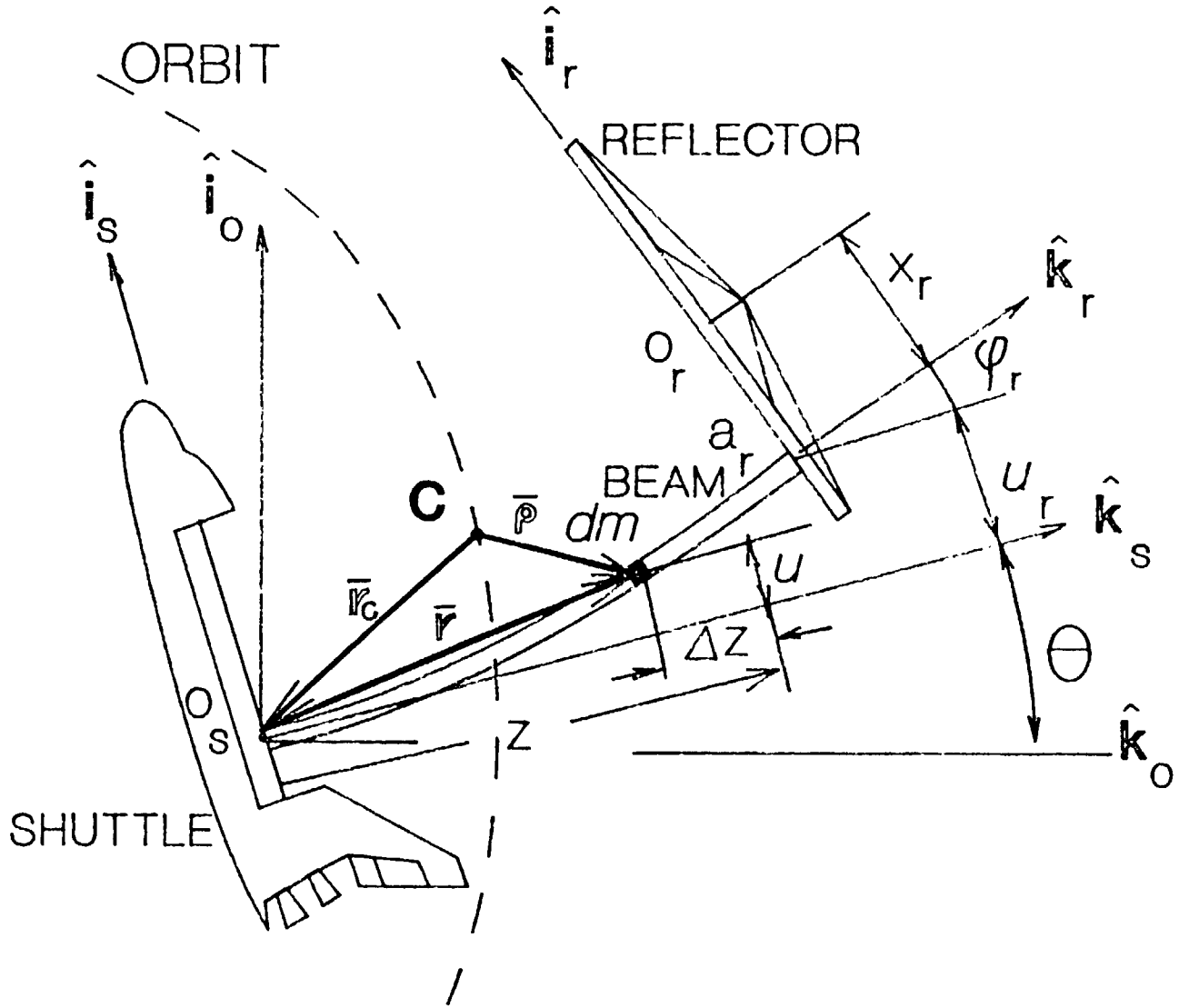

Fig. 1. 2-D Orbiting SCOLE Configuration and Beam Element

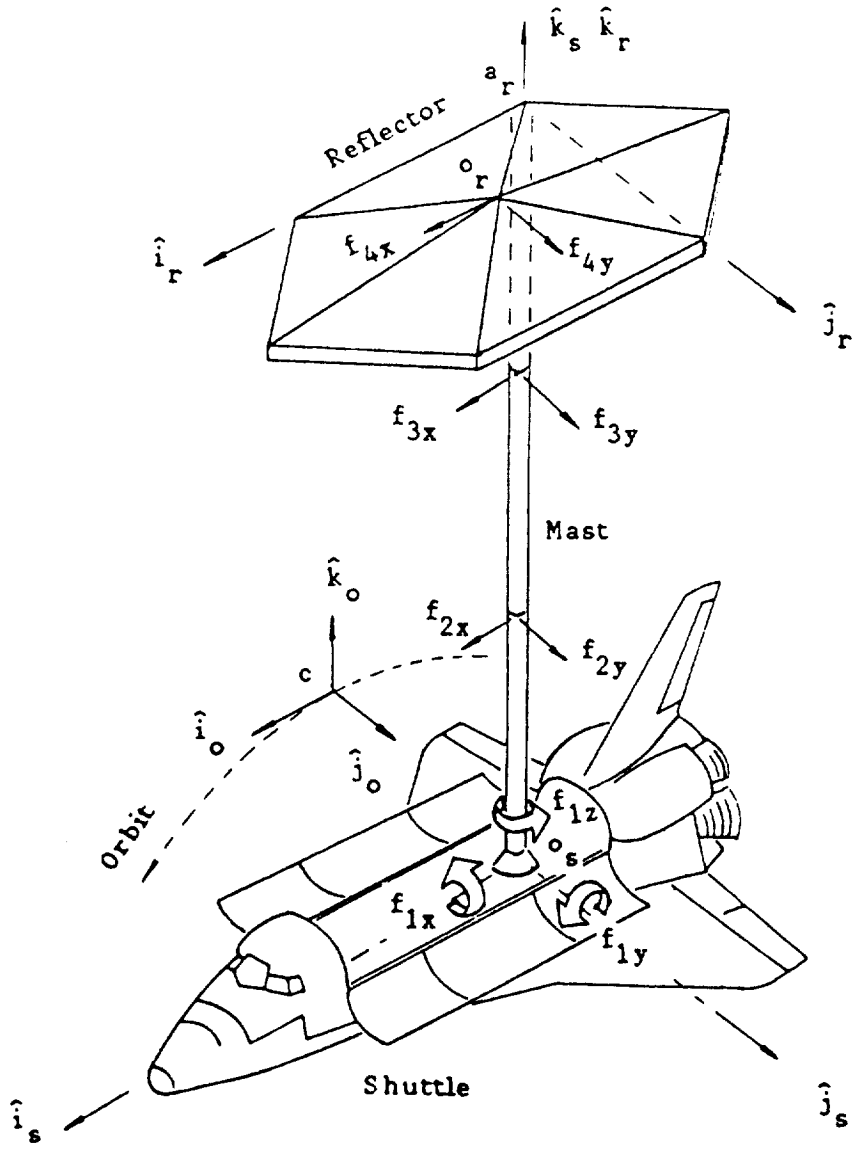

Fig. 2. Drawing of the 3-D Orbiting SCOLE Configuration

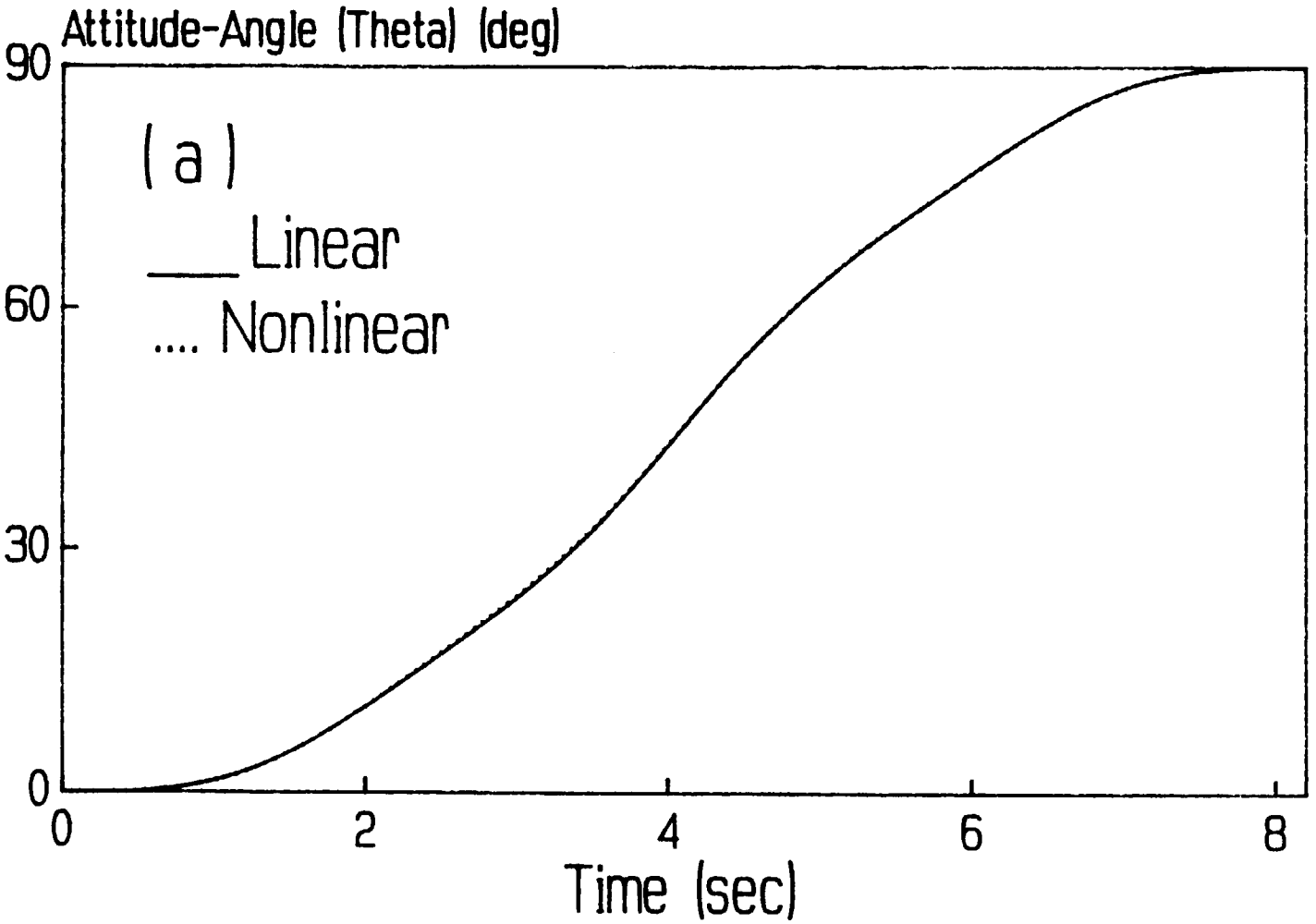

Fig. 3. Results for the 2-D Slew, Case 4: x_f=32.5 ft, $u=[u_1\ u_2\ u_3\ u_4]^T$, t_f=8.196 sec.

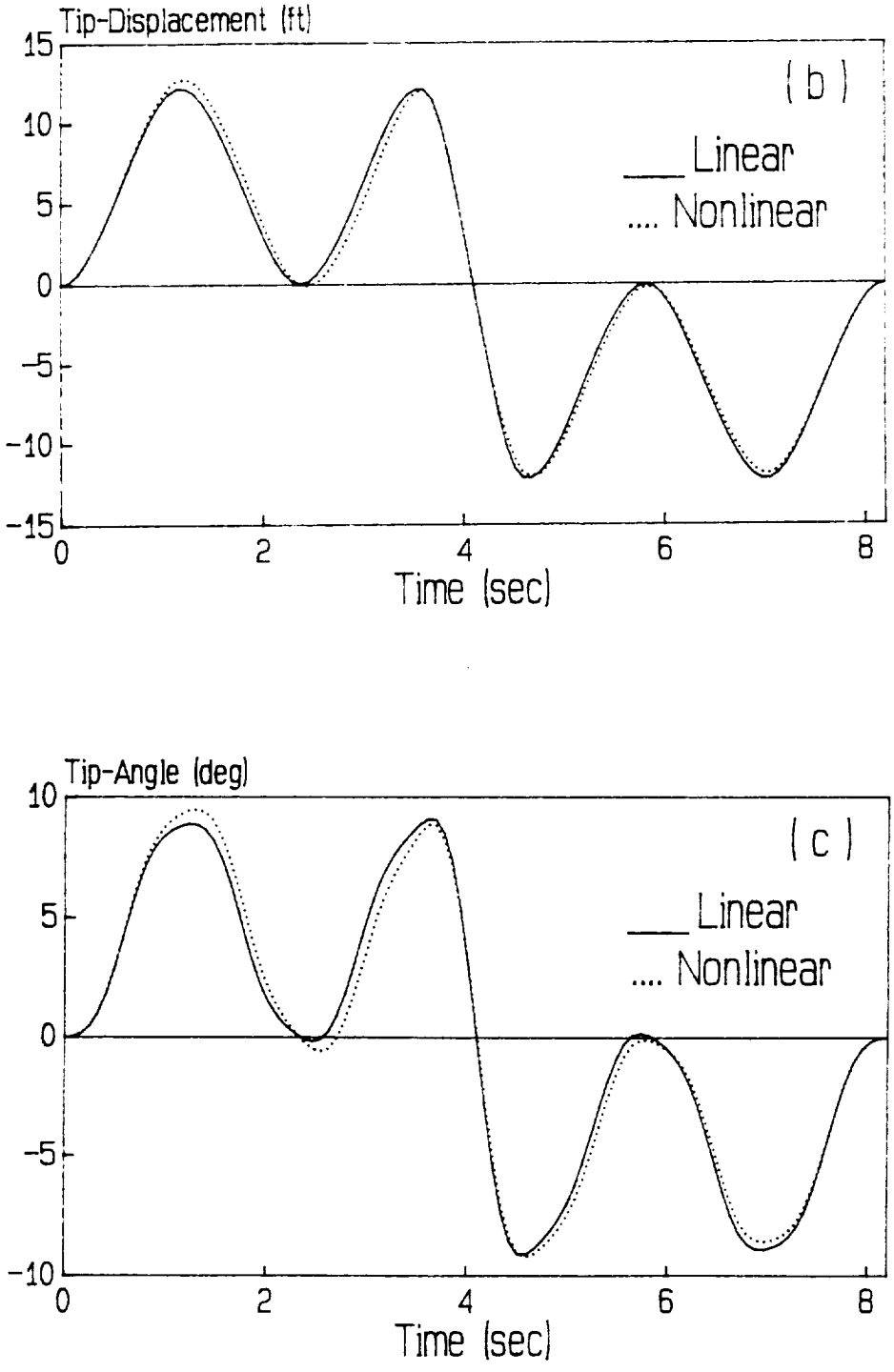

Fig. 3. Results for the 2-D Slew, Case 4: x_r=32.5 ft, $u=[u_1\ u_2\ u_3\ u_4]^T$, t_f=8.196 sec.

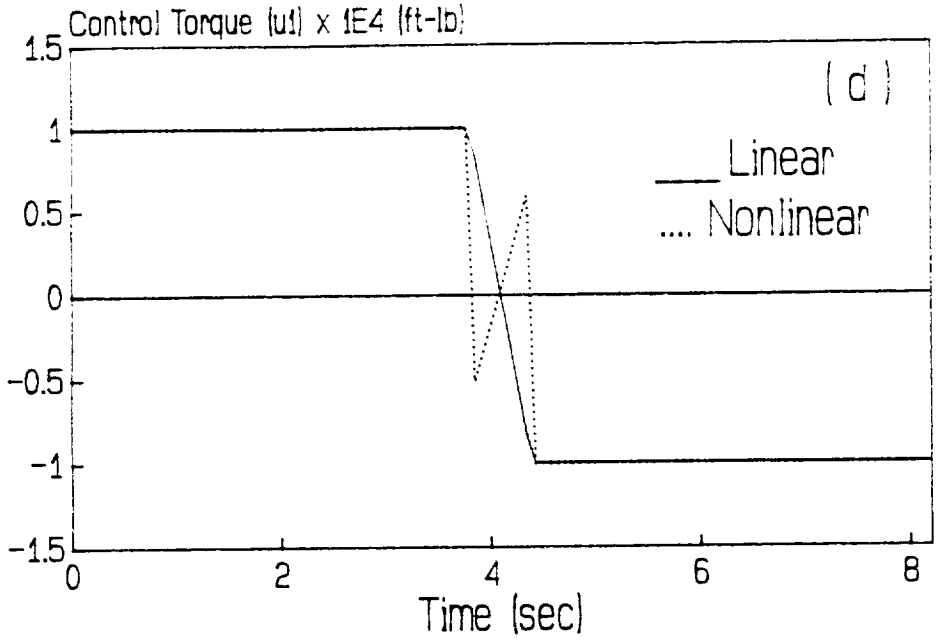

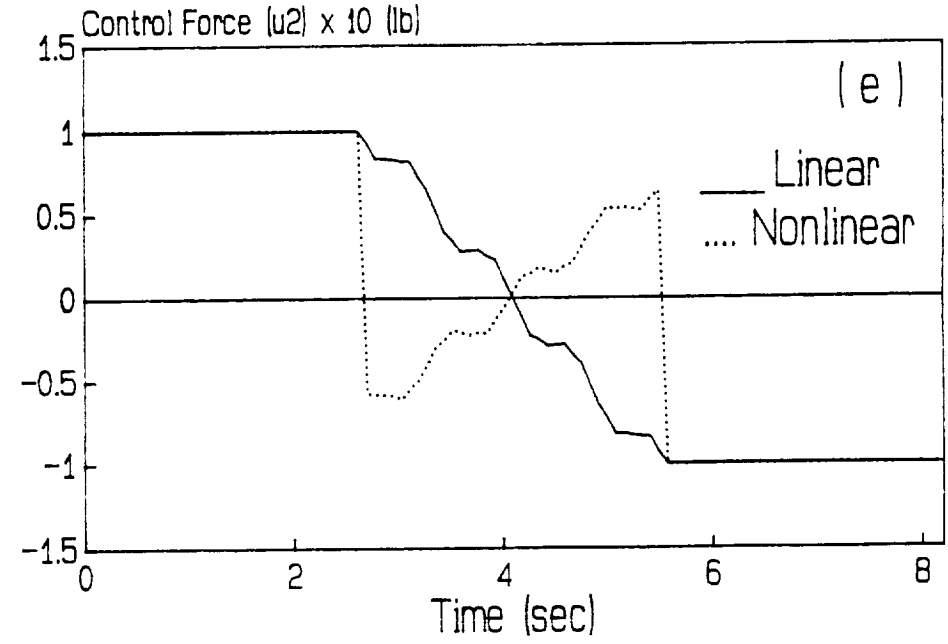

Fig. 3. Results for the 2-D Slew, Case 4: x_r=32.5 ft, $u=[u_1\ u_2\ u_3\ u_4]^T$, t_f=8.196 sec.

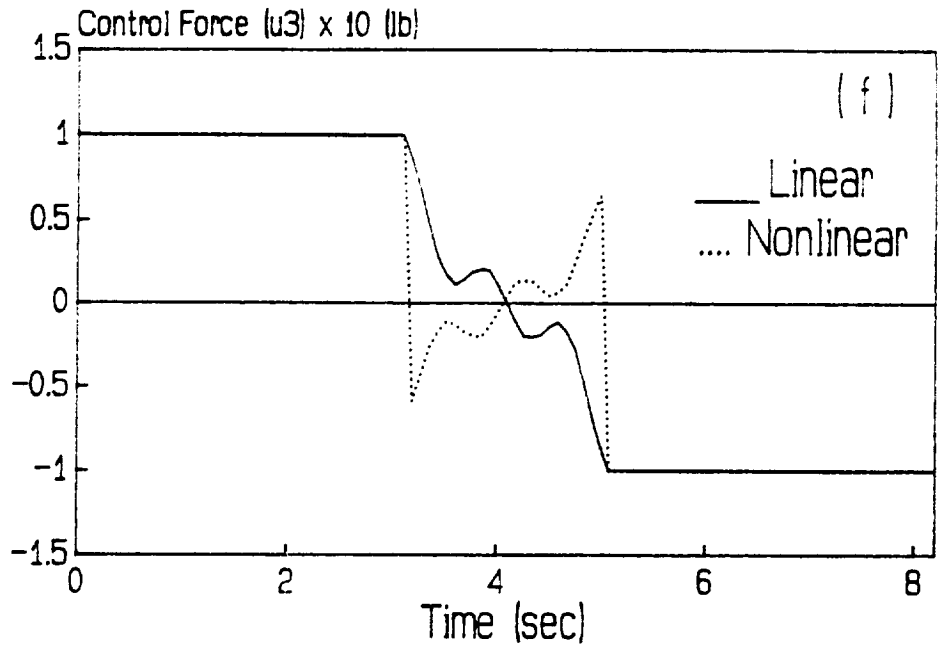

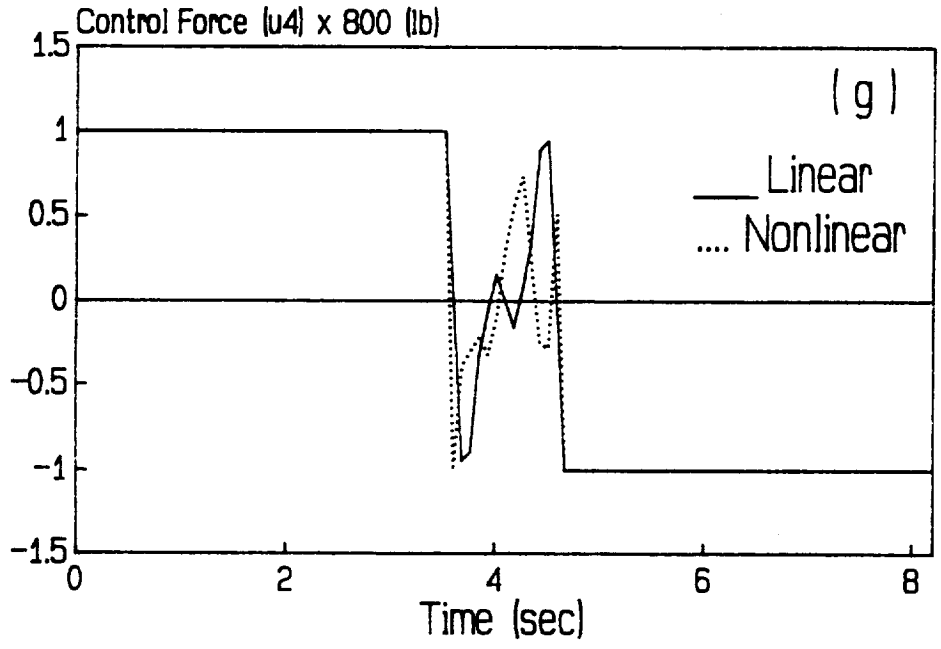

Fig. 3. Results for the 2-D Slew, Case 4: x_r=32.5 ft, $u=[u_1\ u_2\ u_3\ u_4]^T$, t_f=8.196 sec.

Table 1 Tip Displacement and Tip Angle

		Max-Disp (ft)	Min-Disp (ft)	Max-Ang (deg)	Min-Ang (deg)	e-Disp
Case 1	Linearized	0.37727	-0.37727	0.27402	-0.27404	—
$x_r=0$, $\bar{u}=u_1$	$\Delta L=0$, $\omega_0=0$	0.37727	-0.37727	0.27403	-0.27404	0.0%
	$\Delta L\neq 0$, $\omega_0=0$	0.37727	-0.37727	0.27402	-0.27404	0.0%
T=27.6 s	$\Delta L\neq 0$, $\omega_0\neq 0$	0.37728	-0.37728	0.27403	-0.27405	0.0%
Case 2	Linearized	13.072	-13.072	9.6216	-9.6216	—
$x_r=0$, $\bar{u}=\bar{u}$	$\Delta L=0$, $\omega_0=0$	13.186	-13.186	9.7050	-9.7050	0.87%
	$\Delta L\neq 0$, $\omega_0=0$	13.154	-13.154	9.6847	-9.6847	0.63%
T=8.196 s	$\Delta L\neq 0$, $\omega_0\neq 0$	13.153	-13.154	9.6842	-9.6845	0.62%
Case 3	Linearized	0.38812	-0.38812	0.30342	-0.30340	—
$x_r\neq 0$, $\bar{u}=u_1$	$\Delta L=0$, $\omega_0=0$	0.38590	-0.40802	0.29110	-0.33940	5.13%
	$\Delta L\neq 0$, $\omega_0=0$	0.38600	-0.40732	0.29118	-0.33884	4.95%
T=27.6 s	$\Delta L\neq 0$, $\omega_0\neq 0$	0.38586	-0.40803	0.29094	-0.33981	5.13%
Case 4	Linearized	12.191	-12.191	9.1082	-9.1082	—
$x_r\neq 0$, $\bar{u}=\bar{u}$	$\Delta L=0$, $\omega_0=0$	12.734	-12.061	9.4541	-9.1299	4.45%
	$\Delta L\neq 0$, $\omega_0=0$	12.796	-12.052	9.5067	-9.2030	4.96%
T=8.196 s	$\Delta L\neq 0$, $\omega_0\neq 0$	12.795	-12.054	9.5052	-9.2061	4.95%

SOLUTION PROCEDURE FOR NONLINEAR TPBVP

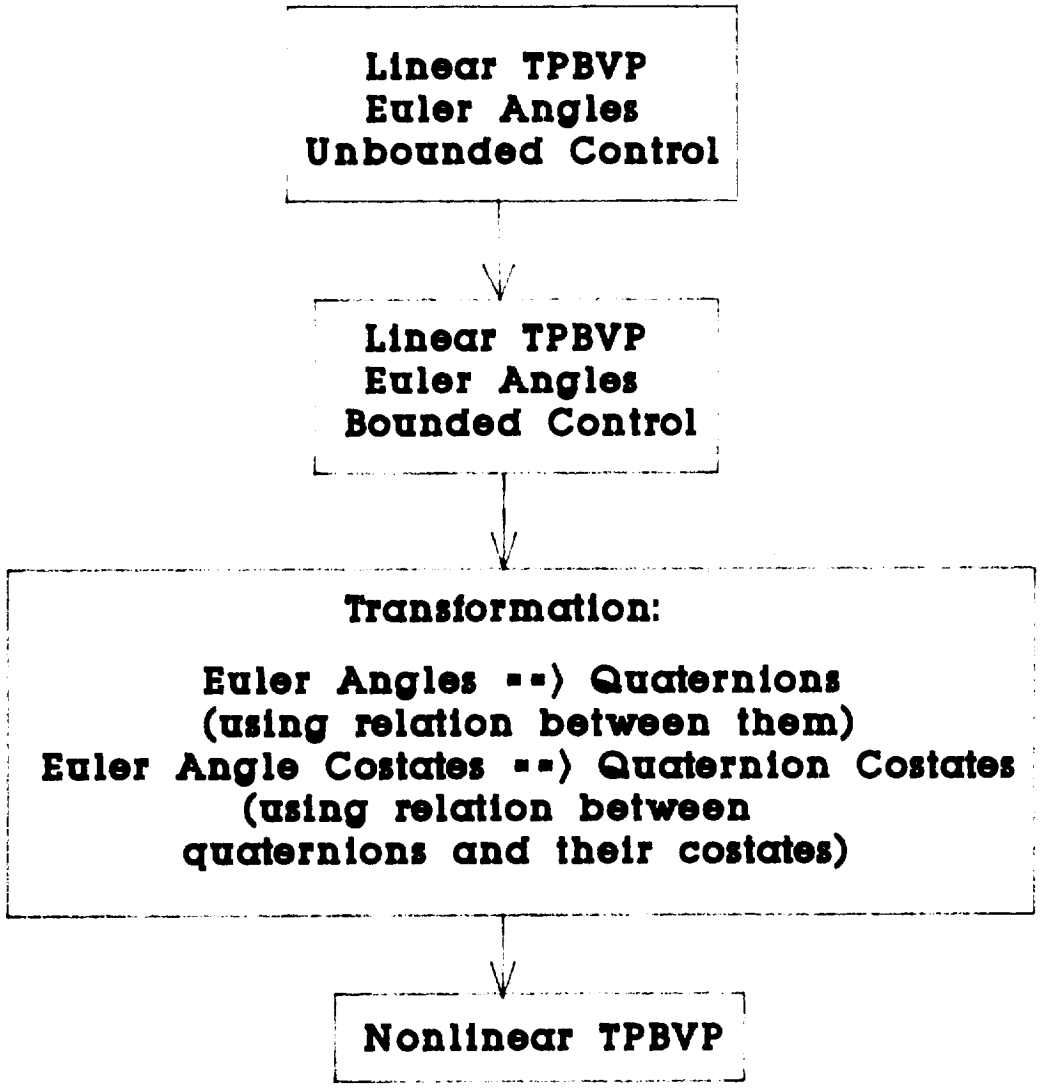

Fig. 4. Solution Procedure for Nonlinear TPBVP

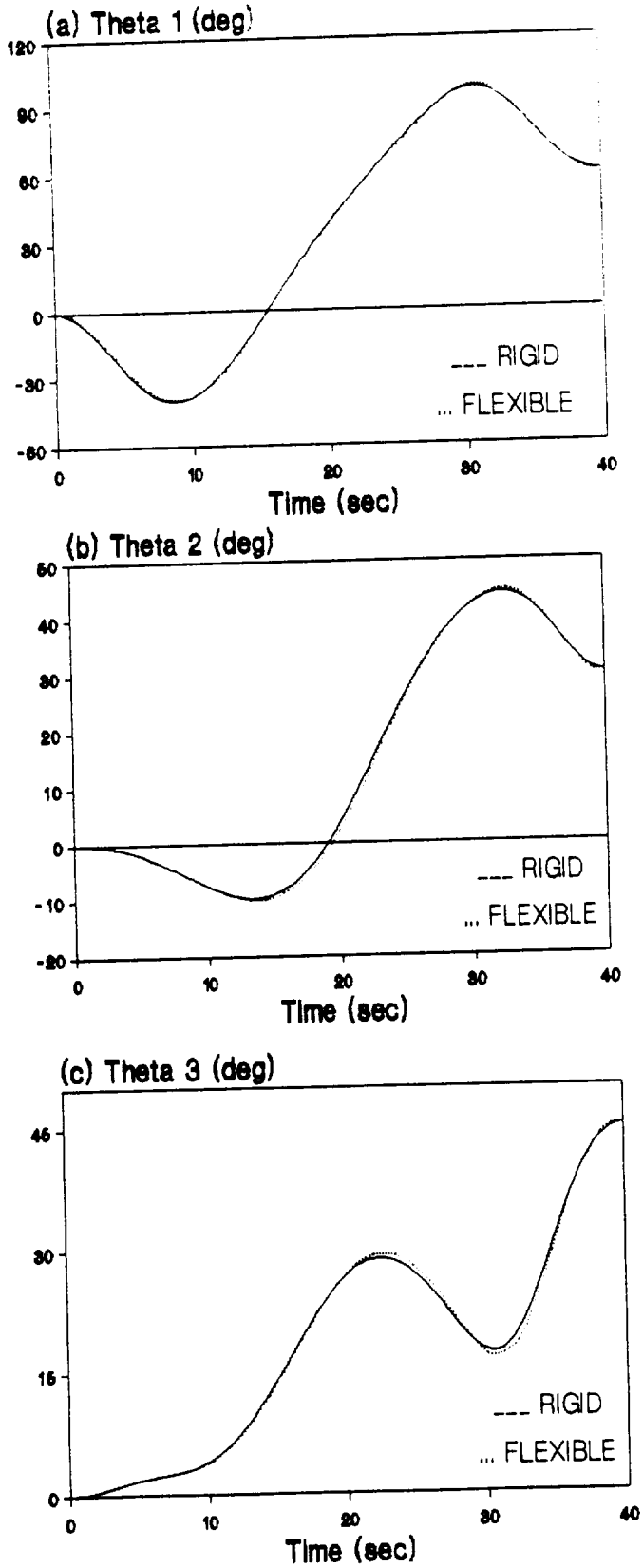

Fig. 5. Results for the 3-D slew, Case 3: 60-30-45 deg-Slew, Shuttle Torques + Reflector Forces, R=Diag(1E-4, 1E-4, 1E-4, 0.6, 1.4E-3).

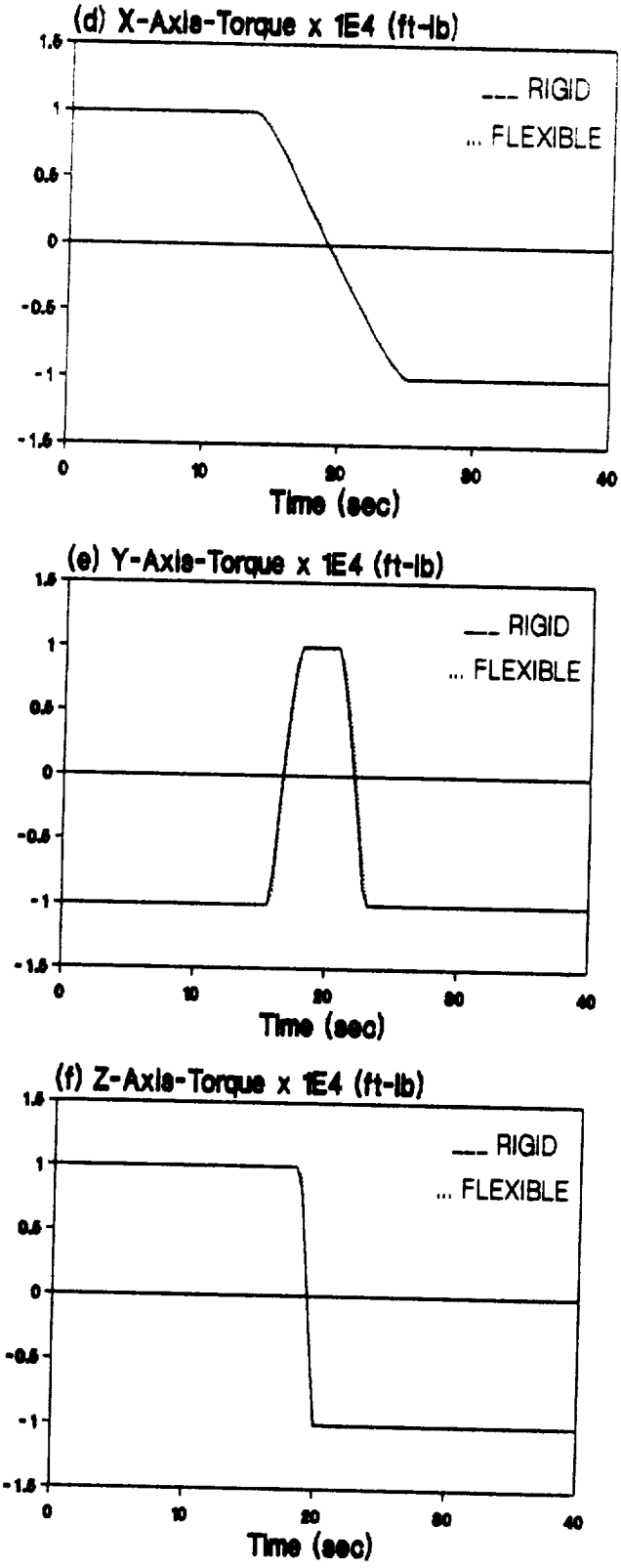

Fig. 5. Results for the 3-D slew, Case 3: 60-30-45 deg-Slew, Shuttle Torques + Reflector Forces, R=Diag(1E-4, 1E-4, 1E-4, 0.6, 1.4E-3).

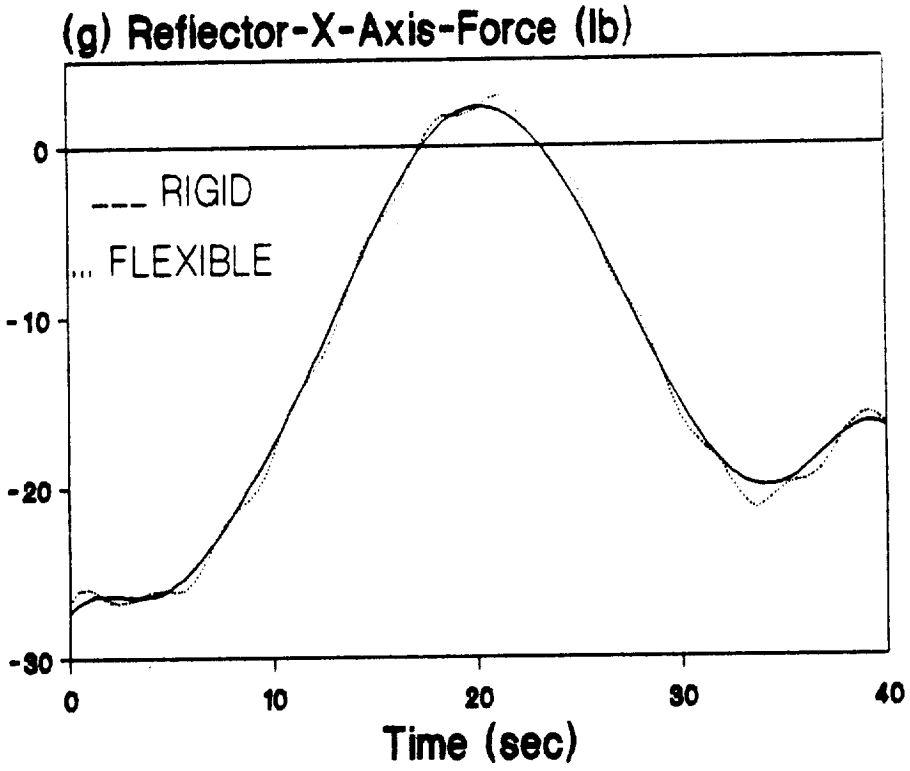

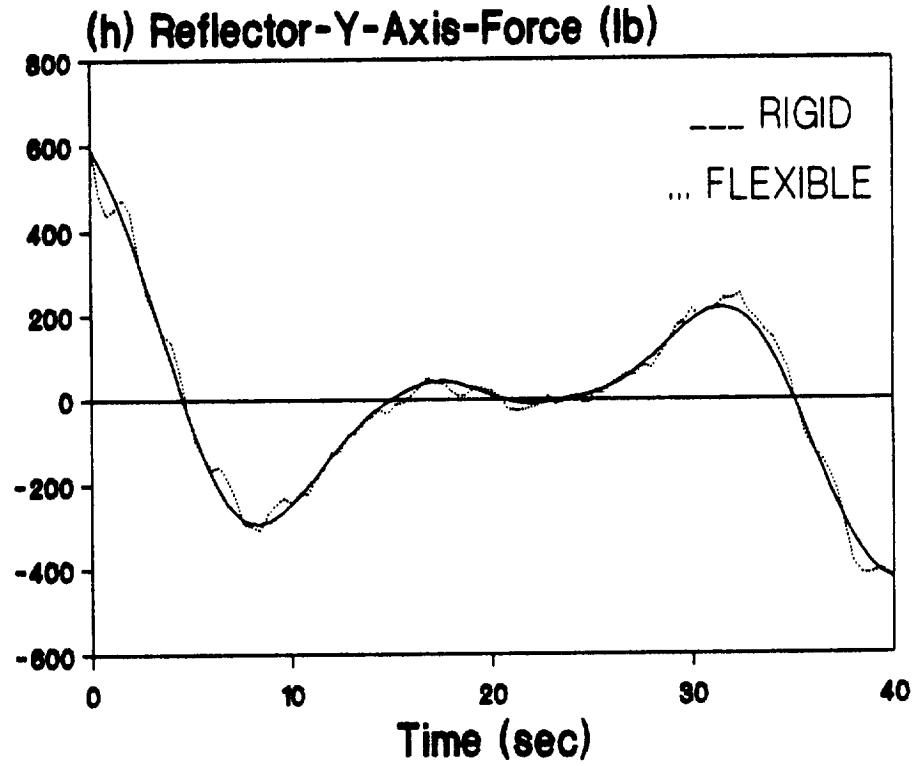

Fig. 5. Results for the 3-D slew, Case 3: 60-30-45 deg-Slew, Shuttle Torques + Reflector Forces, R=Diag(1E-4, 1E-4, 1E-4, 0.6, 1.4E-3).

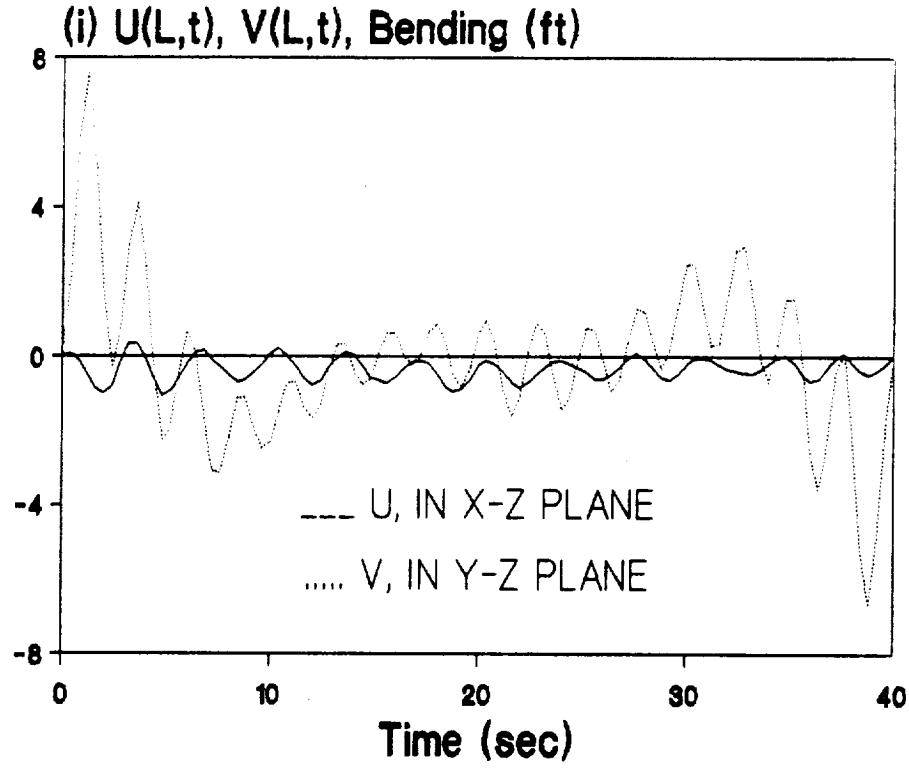

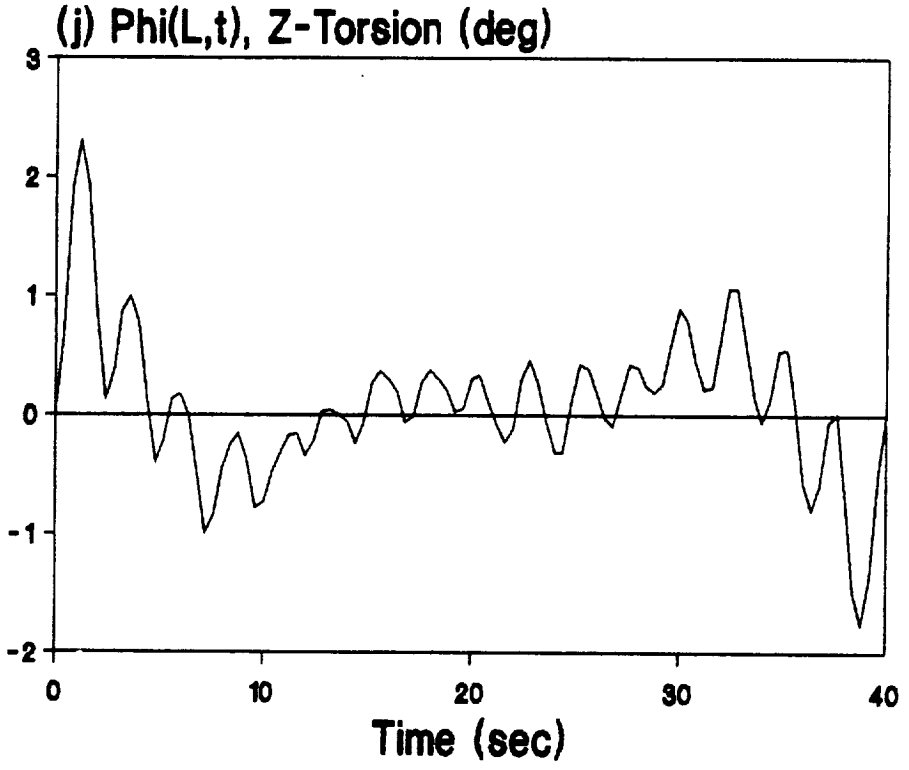

Fig. 5. Results for the 3-D slew, Case 3: 60-30-45 deg-Slew Shuttle Torques + Reflector Forces, R=Diag(1E-4, 1E-4, 1E-4, 0.6, 1.4E-3).